Analytical Biochemistry 626 (2021) 114246

Contents lists available at ScienceDirect

Analytical Biochemistry

journal homepage: www.elsevier.com/locate/yabio

Development of a fluorescence-based assay for screening of urate transporter 1 inhibitors using 6-carboxyfluorescein

Haiyan Zhou [1], Guorui Zhong [1], Jing Bai, Xiaolei Li, Wen Peng, Lei Zhang, Jing Li [*]

MOE International Joint Research Laboratory on Synthetic Biology and Medicines, School of Biology and Biological Engineering, South China University of Technology, Guangzhou, 510006, PR China

ARTICLE INFO

Keywords:
Human urate transporter 1
Hyperuricemia
6-Carboxyfluorescein

ABSTRACT

The urate transporter 1 (URAT1) inhibitors were considered a very promising class of uricosuric agents for the treatment of hyperuricemia and gout. *In vitro* activity testing of these compounds has been conducted by radio-labeling uric acid for a long time. However, relatively few offer the convenience and speed of fluorescence-based assays. Herein, we report the development of a non-radioactive cell-based method for the screening of URAT1 inhibitors using the human embryonic kidney 293T cells stably expressing human URAT1, and 6-carboxyfluorescein (6-CFL) as a substrate. The URAT1-mediated transport of 6-CFL was time dependent and saturable (Km = 239.5 μM, Vmax = 6.2 pmol/well/min, respectively). Molecules known to interact with organic anion transporters, including benzbromarone, probenecid, and lesinurad, demonstrated concentration-dependent inhibition of 6-CFL transport by URAT1. Moreover, we screened a small subset of compounds, and identified compound **4** as a promising URAT1 inhibitor. This *in vitro* assay may be employed to screen for novel URAT1 inhibitors, which are effective against hyperuricemia.

1. Introduction

Approximately 70% of uric acid is mainly excreted via the kidneys, and about 90% of patients with hyperuricemia are urate under-excretors. These data suggest that the regulation of uric acid excretion via the kidneys is a potentially effective therapeutic strategy [1]. In humans, a series of complex transporter systems expressed in the proximal tubules are involved in the process of uric acid excretion and reabsorption. Among them, uric acid transporter 1 (URAT1, SLC22A12) [2], firstly certified as a 12-transmembrane protein in 2002, has been proved to be a specific transporter of uric acid reabsorption, and considered an important target for the management of hyperuricemia [3].

Following the identification of URAT1 in 2002, probenecid, sulfinpyrazone, and benzbromarone – that had already been approved as uricosuric agents – were later found to be UART1 inhibitors [4–8]. However, probenecid is associated with low efficacy [9], short half-life, and side effects such as gastrointestinal irritation and rash [10]. Benzbromarone showed hepatotoxicity, which led to its withdrawal from use in Europe in 2003 [11]. Lesinurad, the first specific UART1 inhibitors developed after 2002, was approved by the United States Food and Drug Administration in 2015 and the European Union in 2016 [12]. However, lesinurad is limited by its low efficacy and narrow therapeutic window [13]. Thus, it is imperative to develop new types of URAT1 inhibitors.

At present, there are two main defects restricting the development of URAT1 inhibitors. Firstly, thus far, there is no report on the URAT1 protein structure, which is not conducive to drug design based on receptor structure. Nevertheless, structural studies on the homologous modeling of URAT1 [9] and 3D-Quantitative Structure Activity Relationship of URAT1 inhibitors [14] have been reported. Secondly, *in vitro* activity test methods for URAT1 inhibitors are currently carried out using radio-labeled uric acid [15]. Although the detection method by radioactive labeling is characterized by high sensitivity and high throughput, the use of radioactive isotopes is costly, and special strict safety precautions should be taken to avoid contamination and ensure appropriate disposal of the waste. In recent years, there is trend toward the development of less polluting alternative methods. Fluorescent-based methods could also provide highly sensitive, quantitative, and high-throughput measures. This approach has yielded numerous excellent *in vitro* evaluation models in the early stage of drug development [16–19]. Therefore, the development of non-radioactive screening methods for URAT1 inhibitors is highly desirable.

* Corresponding author.
E-mail address: lij@scut.edu.cn (J. Li).
[1] These authors contributed equally to this work and should be considered as co-first authors.

https://doi.org/10.1016/j.ab.2021.114246
Received 16 August 2020; Received in revised form 3 February 2021; Accepted 4 May 2021
Available online 7 May 2021

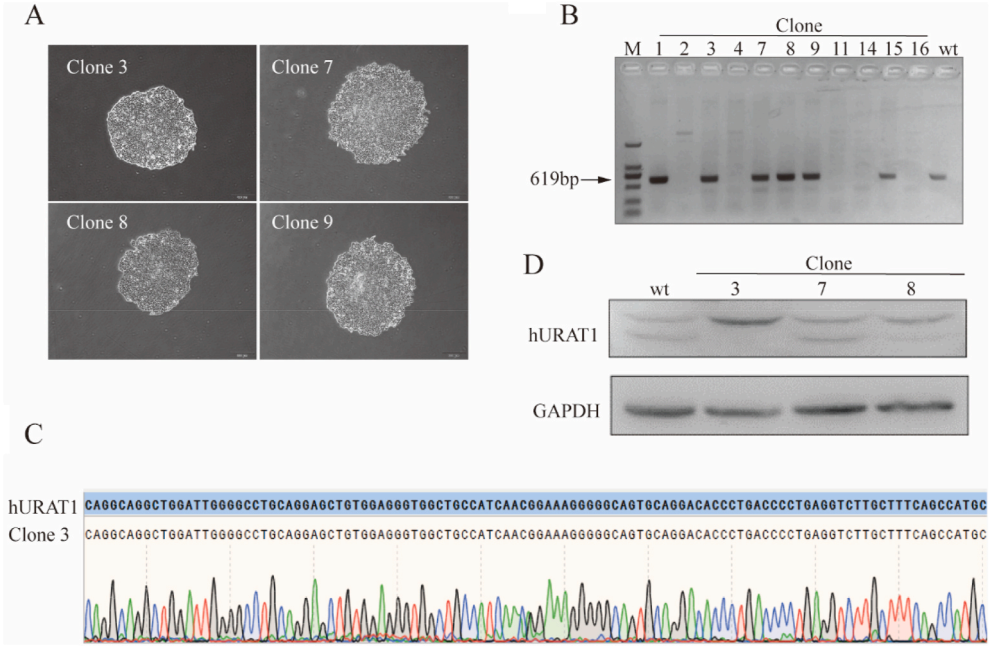

Fig. 1. Development of hURAT1 transgenic HEK293T cell line. (**A**) Representative harvested single-cell colonies. (**B**) PCR analysis of individual colonies. (**C**) Sequencing results of clone 3. (**D**) Western blotting results of clones 3, 7, and 8.
GAPDH, glyceraldehyde-3-phosphate dehydrogenase; HEK, human embryonic kidney; hURAT1, human uric acid transporter 1; PCR, polymerase chain reaction.

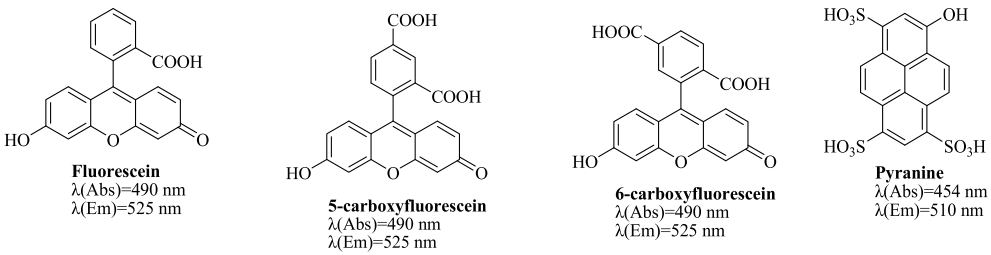

Fig. 2. Fluorescent organic anions and their fluorescence characteristics.

Cihlar et al. revealed that fluorescein and its analogs are frequently used fluorescent substrates, which can be transported by organic anion transporter 1 (OAT1, SLC22A6) [20]. Since OAT1 and URAT1 belong to the same OATs (SLC22 family), we designed and obtained human embryonic kidney 293T cells that stably express human URAT1 (hURAT1), and chose fluorescein and its analogs as potential substrates to develop a non-radioactive cell-based screening system for URAT1 inhibitors. Moreover, URAT1 inhibitors, such as probenecid, benzbromarone, and lesinurad are used in this screening system to evaluate its efficiency and reliability.

2. Materials and Methods

2.1. Materials

All chemical reagents and solvents were purchased from Aladdin (Shanghai, China) and were used directly without any further purification, except for MTT, fluorescein, 5-carboxyfluorescein (5-CFL), 6-carboxyfluorescein (6-CFL) and 8-hydroxypyrene-1,3,6-trisulfonic acid (pyranine), which were obtained from Sigma–Aldrich (St. Louis, MO, USA). Compounds **1**–**12** were obtained from our lab's own library of compounds.

2.2. Construction of hURAT1 expression vectors

The hURAT1 cDNA (Genbank ID: 116085) was amplified and subsequently cloned into a pCMV vector using a restriction site for EcoRI and XhoI. Plasmids for cell transfection were prepared using an Endo-free Plasmid Mini kit (Omega Bio-Tek, Norcross, GA, USA).

2.3. Cell culture and transfection

293T cells were obtained from the American Type Culture Collection and cultured in Dulbecco's Modified Eagle's Medium (DMEM) supplemented with 10% fetal bovine serum (Gibco, Australia), 2 mM L-glutamine, 100 U/mL penicillin, and 100 μg/mL streptomycin in a humidified atmosphere with 5% CO_2 at 37 °C.

Prior to transfection, 0.1×10^6 293T cells were seeded into 24-well plates (Corning Inc., Corning, NY, USA). When cultures reached 70–80% confluence, cells were transfected with 0.5 μg linearized CMV-hURAT1 plasmid using the GenJet™ In Vitro DNA Transfection Reagent (SignaGen, Rockville, MD, USA) according to the instructions provided by the manufacturer.

2.4. Establishment of isogenic 293T cell lines stably expressing hURAT1 by monoclonal expansion

At 48 h post transfection, transfected 293T cells were seeded onto 10-

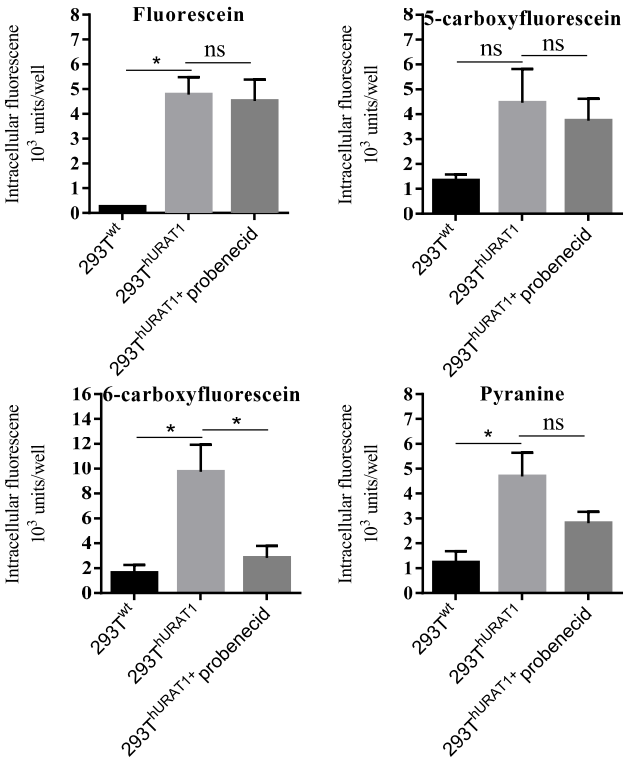

Fig. 3. Transport of fluorescent organic anions by hURAT1. 293T ^{hURAT1} and 293T^{wt} cells in 96-well plates were incubated in the presence of various fluorescent anions at 50 μM concentration. Where indicated, 1 mM probenecid was added together with the tested compound. After 60 min of incubation at room temperature, the cells were washed and lysed. The cell-associated fluorescence was determined as described in the Materials and Methods section. The panels show mean values ± standard errors from two independent experiments performed in triplicate.
hURAT1, human uric acid transporter 1.

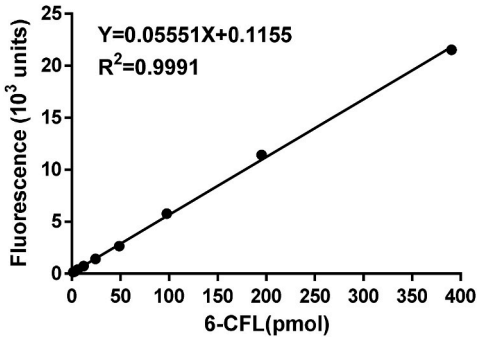

Fig. 4. Calibration curve of the 6-CFL fluorescent signal. Various amounts of 6-CFL were added to 100 μL of cell lysis buffer, and the fluorescent signal was determined. The data are the means from two experiments performed in triplicate.

cm dishes at a low density (20 cells per dish) and cultured with selective medium (1 μg/mL puromycin). The culture medium was changed every 2 days. After 8–10 days of selection, puromycin-resistant cell colonies were isolated using cloning rings for monoclonal expansion and further cultured on 24-well plates. When selected colonies reached confluence, genomic DNA was extracted from individual cells using the Takara Mini BEST Universal DNA Extraction Kit (Takara, Kusatsu, Japan) according to the instructions provided by the manufacturer. The URAT1 region was amplified via polymerase chain reaction (PCR) with primers P1/P2. The primer sequences were as follows: (P1) 5′-ATGGCCCAGTCCATCTACCT-3'; (P2) 5′-GAGATACAGGTCCGGAAGCG-3'. PCR products of colonies were subjected to sequencing, and integration was confirmed using the Basic Local Alignment Search Tool to search against the hURAT1 genome.

2.5. Western blotting

Protein samples were homogenized in lysis buffer containing protease inhibitors. Lysates were centrifuged at 1,000 g and supernatants were centrifuged at 10,000 g for 90 min. Membrane protein content was determined using the BCATM Protein Assay Kit (Shanghai, China), which is based on the biuret reaction. Membrane proteins were subjected to electrophoresis on a 12% sodium dodecyl sulfate-polyacrylamide gel and electrophoretically transferred onto polyvinylidene difluoride membranes. The blots were subsequently blocked overnight at 4 °C with phosphate-buffered saline containing 5% nonfat dry milk powder and 1% bovine serum albumin. After washing thrice with phosphate-buffered saline, the proteins were hybridized for 75 min at room temperature with the polyclonal rabbit antibody against URAT1 in 293T cells (dilution 1:1,000 in blocking buffer). Subsequently, the blots were incubated with a secondary anti-rabbit-horseradish peroxidase-conjugated antibody (ICLLAB, USA) for 1 h at room temperature, followed by enhanced chemiluminescence detection.

2.6. Fluorescent transport assay

293T^{hURAT1} or 293T^{wt} cells were seeded into 96-well plates at a density of 4×10^4 cells per well. After 48 h, the cells were washed thrice with Hank's balanced salt solution (HBSS) and incubated at room temperature in the presence of transport medium (HBSS containing HEPES [25 mM] and glucose [10 mM]; pH 7.4) containing the fluorescent substrate. Cellular uptake was terminated by washing the wells thrice with 200 mL ice-cold HBSS. Subsequently, the cells were lysed with 100 μL of 0.5 N NaOH for 30 min at room temperature. The fluorescence was determined using a SpectraMax Gemini 96-well plate fluorescence reader (Molecular Devices, Sunnyvale, CA, USA). To determine the 50% inhibitory concentration (IC_{50}) values in the inhibition assay, two-fold serial dilutions of the tested compounds were prepared in triplicate in a separate 96-well plate and mixed with an equal volume of 478.9 μM 6-CFL. The uptake was initiated by addition of the premixed samples to HBSS-washed cells. The final concentration of substrate in the assay was equal to its Km (239.5 μM). The incubation lasted 60 min at room temperature, followed by intracellular fluorescence determination as above.

2.7. MTT assay

The 293T^{hURAT1} cells were seeded at 4×10^4 per well. Following 48 h of incubation, the test compounds were added to the plates. The plates were incubated at 37 °C. After 1 h, cellular uptake was terminated by washing the wells thrice with 200 mL HBSS. DMEM complete medium containing 2% fetal bovine serum was used to prepare the MTT solution (5 mg/mL diluted to 0.5 mg/mL), and 100 μL were added to each well. The plates were incubated for 4 h. Subsequently, the MTT solution was aspirated, 200 μL of dimethyl sulfoxide solution was added to each well, the plate was shaken on a microplate reader for 10 min, and read at an ultraviolet wavelength of 490 nm. Finally, the survival rate of cells was calculated.

3. Results and discussion

3.1. Generation of URAT1-expressing cells

293T cells were transfected with the pCMV-hURAT1 plasmid. After 7–8 days of puromycin selection, 18 colonies were selected and seeded into 24-well plates. Seventeen colonies reached confluence and were

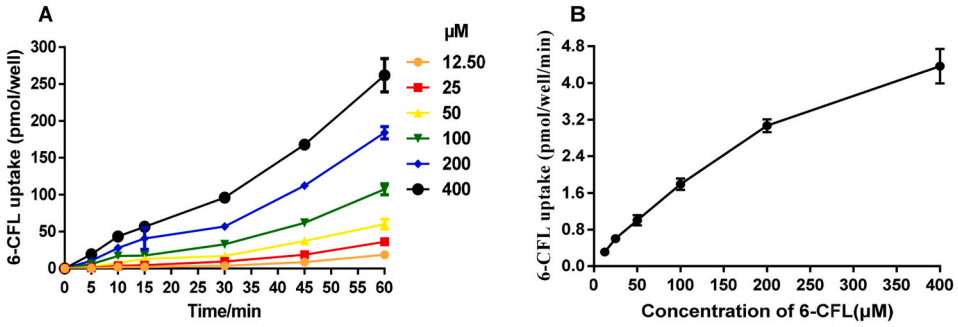

Fig. 5. Kinetics of 6-CFL transport mediated by hURAT1. (**A**) Time course of hURAT1-specific uptake of 6-CFL. The plot shows the mean values from a representative experiment performed in triplicate. (**B**) Saturation curve of the hURAT1-specific uptake of 6-CFL at the 60-min time point.

Table 1
IC_{50} of the three URAT1 inhibitors obtained by the test system in this study and radioactive methods reported in the literature.

Inhibitor	IC_{50} (μM)[a]	IC_{50} (μM)[b]
Probenecid	22 ± 8.77	1518.67 ± 8.08
Benzbromarone	0.29 ± 0.07	14.25 ± 4.96
Lesinurad	7.3 ± 3.8	273.5 ± 35.47

IC_{50}, 50% inhibitory concentration.
[a] Literature values obtained by the radioscopy assay [10,12].
[b] Values of the present study.

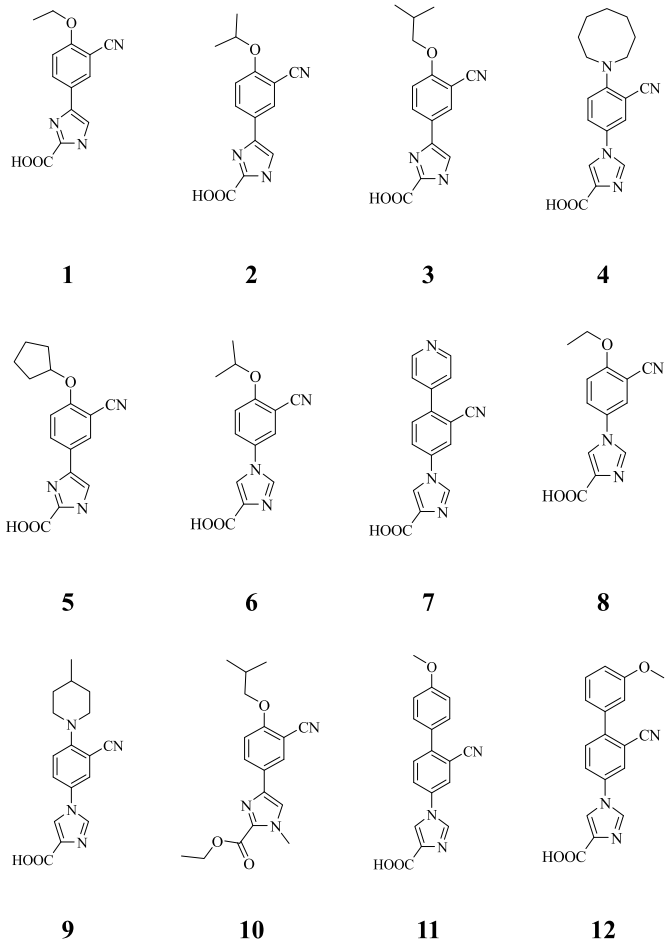

Fig. 6. The structures of compounds **1**–**12**.

identified by PCR analysis (Fig. 1A). Eleven colonies (64.7%, 11/17) showed stably integrated URAT1 (Fig. 1B). Sanger sequencing further confirmed that URAT1 was integrated with no indel mutation for clone 3 (Fig. 1C). The expression of URAT1 in clones 3, 7, and 8 was confirmed by western blotting analysis. Compared with wild-type 293T cells, URAT1 protein was expressed at a significantly higher level in clone 3 (Fig. 1D). These results suggest that the 293T-hURAT1-expressing cell lines were successfully generated. Clone 3 was chosen for further 6-CFL transport study.

3.2. Transport of fluorescent organic anions by hURAT1

A previous study demonstrated that renal proximal tubules are able to accumulate fluorescein [21]. This accumulation was inhibited by probenecid and various organic anions, suggesting that fluorescein and possibly some other fluorescent anions may be substrates for hURAT1; thus, they may serve as potential probes to assess hURAT1 transport activity. Therefore, those fluorescent organic anions, fluorescein, 5-CFL, 6-CFL, and pyranine, were evaluated for their hURAT1-mediated transport in 293T ^{hURAT1} cells. Their structures and parameters used to determine their fluorescent signal are presented in Fig. 2. Fluorescein, 5-CFL, 6-CFL, and pyranine showed approximately 19-, 3-, 7-, and 4-fold higher fluorescence intensity in 293T^{hURAT1} cells than in control 293T^{wt} cells, respectively (Fig. 3). When 5-CFL was used as substrate, there was no significant difference in fluorescence intensity between 293T^{hURAT1} cells and 293T^{wt} cells ($P > 0.05$), indicating that the transgenic protein URAT1 expressed by the transgenic cells is specifically bound to fluorescein, 6-CFL, and pyranine. In the presence of probenecid, the fluorescence intensity of fluorescein, 5-CFL, and pyranine in 293T^{hURAT1} cells did not exhibit significant difference compared with that detected in 293T^{wt} cells ($P > 0.05$). In contrast, the fluorescence intensity of 6-CFL in the probenecid-added 293T^{hURAT1} cells was markedly decreased compared with that observed in 293T^{hURAT1} cells without probenecid ($P < 0.05$). This finding suggested that probenecid (as a URAT1 inhibitor) interferes with the transport of 6-CFL by URAT1. Hence, 6-CFL can be regarded as the specific transport substrate of URAT1. In addition, in the presence of probenecid, the fluorescence intensity in 293T^{hURAT1} cells was not significantly different from that of 6-CFL in 293T^{wt} cells ($P > 0.05$). Probenecid completely inhibits the uptake of 6-CFL by URAT1 transport in 293T^{hURAT1} cells, indicating that the transport of 6-CFL is URAT1-specific in this cell line.

Those fluorescent organic acids could be regarded as hURAT1 substrates since their fluorescence intensity in 293T ^{hURAT1} cells is 3- to 20-fold higher than that detected in 293T^{wt} cells. Furthermore, an efficient hURAT1-specific transport of 6-CFL was noted in 293T ^{hURAT1} cells. Collectively, these results suggested that 293T^{hURAT1} cells with 6-CFL as fluorescent substrate may be used to develop an assay for the evaluation of the affinity of tested compounds toward hURAT1.

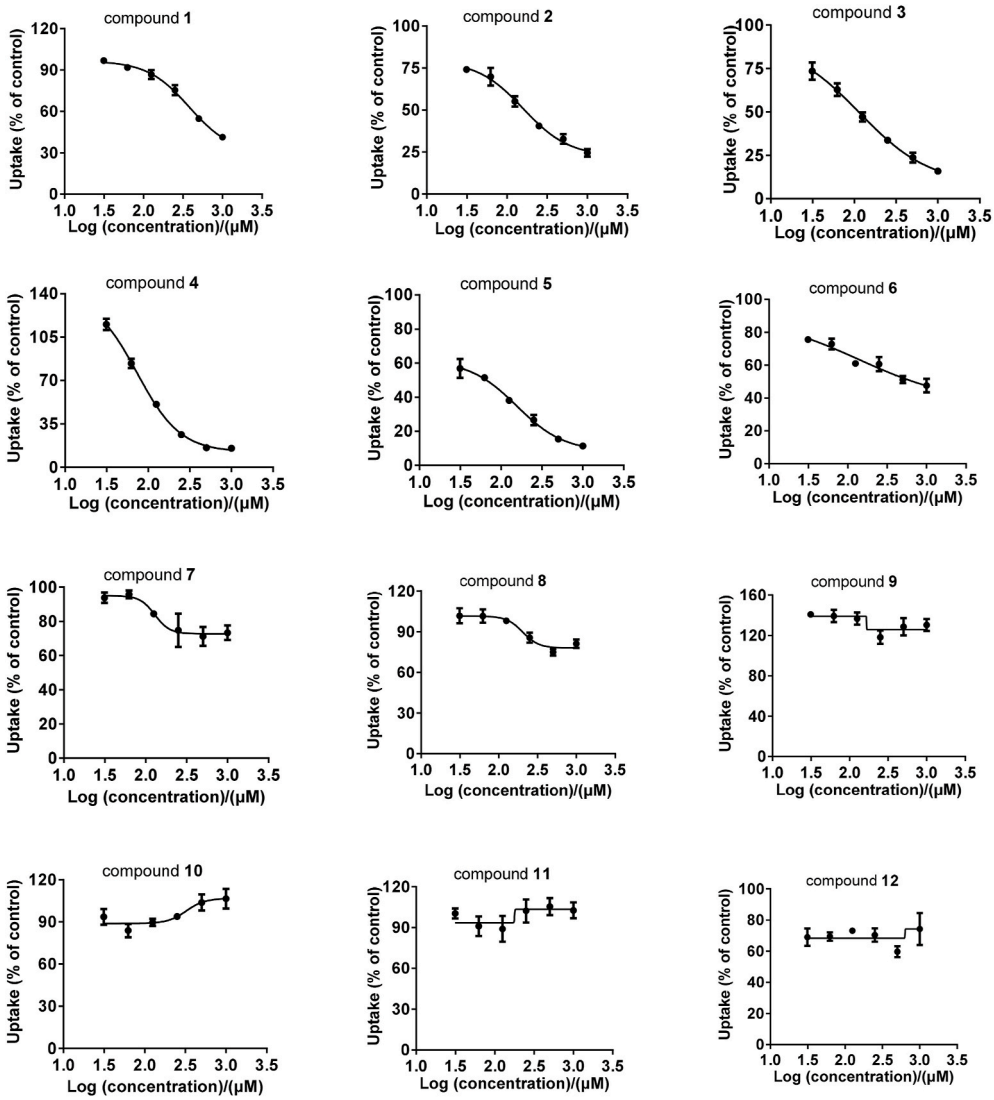

Fig. 7. Inhibitory effects of test compounds on URAT1-mediated uptake of 6-CFL. Uptake of 6-CFL (239.5 μM) mediated by URAT1 was examined for 60 min at 37 °C in the presence or absence of these compounds (concentration: 31.25–1,000 μM). Solid lines represent fitted lines for the inhibition of 6-CFL uptake by the inhibitors, obtained by a nonlinear least-squares regression analysis. Each point represents the mean ± SD (n = 3).

Table 2
IC_{50} values of the test compounds for URAT1.

Compd.	IC_{50}/μM	Compd.	IC_{50}/μM
1	656.83 ± 135.35	**9**	-
2	154.5 ± 5.97	**10**	-
3	113.65 ± 11.02	**11**	-
4	10.82 ± 5.50	**12**	-
5	159.57 ± 62.51	Probenecid	1,518.67 ± 8.08
6	172.96 ± 67.02	Benzbromarone	14.25 ± 4.96
7	-	Lesinurad	273.5 ± 35.47
8	-		

$IC_{50,}$ 50% inhibitory concentration; URAT1, uric acid transporter 1.

3.3. Characterization of 6-CFL transport by hURAT1

As demonstrated by the calibration curve in Fig. 4, the fluorescent intensity of 6-CFL in the cell lysis buffer showed a linear increase ranging 1.5–390 pmol. To determine the affinity of 6-CFL toward hURAT1, the kinetic parameters of the 6-CFL transport process mediated by URAT1 were analyzed. The high efficiency and low background of hURAT1-mediated transport of 6-CFL allowed these experiments to be performed in 96-well plates at room temperature. Firstly, a time course of hURAT1-specific uptake of 6-CFL at various concentrations ranging 12.5–400 μmol/L was determined. Fig. 5A illustrates the intracellular accumulation of 6-CFL via hURAT1, showing an approximately linear time dependence upward from 0 min to 15 min. The increase in the curve began to markedly slow down, and this state lasted for 30 min; this was followed by a linear upward trend which continued until the end of the test. The curve with a concentration of 6-CFL at 12.5 μmol/L between 0 to 15 min and 30–60 min was chosen for linear regression; the slope of the curve during these time points was approximately 5.0 and 5.6 pmol/well/min, respectively. The Vmax and Km was also calculated at the endpoint (60 min), obtaining values of 6.2 pmol/well and 239.5 μmol/L respectively; these data indicated that the most appropriate incubation time in the assay was 60 min. Fig. 5B was obtained based on the concentration as the abscissa and the 6-CFL uptake as the ordinate at 60 min. In Fig. 5B, it is evident that, in response to the increase in the concentration of 6-CFL, the absorption rate of $293T^{hURAT1}$ cells for 6-CFL gradually decreased and tended toward saturation. Therefore, 6-CFL was determined as the substrate with an incubation concentration of 239.5 μmol/L and incubation time of 1 h in $293T^{hURAT1}$ cells for the *in vitro* screening of URAT1 inhibitors.

6-CFL, 6-carboxyfluorescein.

6-CFL, 6-carboxyfluorescein; hURAT1, human uric acid transporter 1.

3.4. URAT1 inhibition assay with 6-CFL as the fluorescent substrate

URAT1 inhibitors (benzbromarone, probenecid, and lesinurad) were used to perform *in vitro* fluorometry. Firstly, the MTT assay of those URAT1 inhibitors in 293T^{hURAT1} cells was performed to determine the dosage of each compound when the cell survival rate was >75%, which could be regarded as the maximum dosage in the URAT1-mediated 6-CFL uptake assay. The IC_{50} values for benzbromarone, probenecid, and lesinurad obtained using this assay were 14.25 ± 4.96 μmol/L, 1,518.67 ± 8.08 μmol/L, and 273.5 ± 35.47 μmol/L, respectively (Table 1). Based on the reported IC_{50} values for these three inhibitors by ^{14}C-uric acid-based radioscopy, benzbromarone was the most effective inhibitor. Lesinurad exhibited moderate inhibitory activity, and probenecid showed relative weak inhibition in the fluorometry assay, which is consistent with the trend noted in the radioscopy assay. However, the IC_{50} values measured using our fluorometry method were expanded by two orders of magnitude for all three inhibitors. This may be due to the insufficient affinity of 6-CFL for URAT1; hence, it is necessary to increase the dosage of the compound to be measured to detect the change in fluorescence intensity. Therefore, further investigation on the modification of the fluorescent substrate is warranted.

The 6-CFL-293T^{hURAT1} cell fluorometry system was also used to perform a preliminary novel URAT1 inhibitor screening. The structures of compounds **1**–**12** [22] are shown in Fig. 6 and the results are illustrated in Fig. 7. Within the concentration range (31.25–1,000 μM), the inhibitory effect of compounds **1**–**9** gradually increased in parallel with the concentration. When the concentration of compounds **7**–**9** ranged 250–1,000 μM, the entire curve tended to be saturated. When the concentration reached 1,000 μM, the inhibitory effect did not reach 50%. This indicated that, although these compounds have a certain affinity for URAT1, their inhibitory efficacy is insufficient. Even if the concentration continues to increase, it cannot completely inhibit the transport of 6-CFL by URAT1; thus, compounds **7**–**9** can be regarded as partial antagonists. Compounds **10** and **11** showed a certain inhibitory effect at concentrations of 31.25–125 μM. However, when the concentration increased beyond 125 μM, the inhibitory of 6-CFL was reversed to promote the uptake of 6-CFL by URAT1. This special mechanism suggests that these two compounds may exert a bidirectional regulatory effect on the transport function of URAT1. Compound **12** is special because it exhibits poor affinity and weak potency.

6-CFL, 6-carboxyfluorescein; IC_{50}, 50% inhibitory concentration; SD, standard deviation; URAT1, uric acid transporter 1.

The IC_{50} value of each compound for URAT1 was calculated, as shown in Table 2. Benzbromarone is currently the most active compound *in vitro*. We found that the IC_{50} value of compound **4** (IC_{50} = 10.82 ± 5.50 μM) was similar to that of benzbromarone (IC_{50} = 14.25 ± 4.96 μM), indicating that this compound may be a URAT1 inhibitor with strong inhibitory potential. Lesinurad (IC_{50} = 273.5 ± 35.47 μM) is a URAT1 inhibitor with moderate inhibitory activity. Compounds **2** (IC_{50} = 154.5 ± 5.97 μM), **3** (IC_{50} = 113.65 ± 11.02 μM), **5** (IC_{50} = 159.57 ± 62.51 μM), and **6** (IC_{50} = 172.96 ± 67.02 μM) showed stronger inhibitory activity than lesinurad ($P > 0.05$), suggesting that these compounds may also be potential URAT1 inhibitors. Collectively, these results indicate that our non-radioactive system using 6-CFL is valid for the screening of selective URAT1 inhibitors.

4. Conclusion

URAT1 inhibitors are a class of drugs with broad prospects in the current anti-hyperuricemia and anti-gout drug market. For the development of new highly efficacious and safe drugs, it is important to evaluate the inhibitory potencies of synthesized compounds against URAT1 from the early stage of drug development, For the purpose of high-throughput screening, the use of fluorescence-based *in vitro* assays is preferable. This study was designed to identify fluorescent URAT1 probe substrates, which are readily available from commercial sources and applicable to the development of fluorescence-based URAT1 inhibition assays.

We successfully used 6-CFL to set up a non-radioactive cell-based platform for the screening of URAT1 inhibitors. The use of 6-CFL instead of isotope-labeled ^{14}C-uric acid is safer, more cost-effective, and convenient. This platform may be used to screen selective URAT1 inhibitors from either synthetic compounds or herbal extracts in the current 96-well format. This approach can be further developed into a high-throughput screening system. We screened a small subset of compounds in our laboratory; among those, compound **4** was suggested to be a URAT1 inhibitor with strong inhibitory potential. Although 6-CFL is not the best fluorescence substrate, future investigation will focus on optimizing this assay. This system should provide a rapid and reliable method for the development of novel therapeutic agents against hyperuricemia.

Credit author statement

Haiyan Zhou: Writing-Original draft preparation, Do the fluorescent transport assay, Do the MTT assay, Methodology, Data analysis.

Guorui Zhong: Writing-Original draft preparation, Construction of hURAT1 expression vectors, Methodology, Data analysis.

Jing Bai: Establishment of isogenic 293T cell lines stably expressing hURAT1 by monoclonal expansion.

Xiaolei Li: Synthesis of 12 compounds to be tested.

Wen Peng: Writing-Reviewing and Editing.

Lei Zhang: Visualization, Validation.

Jing Li: Writing-Reviewing and Editing, Supervision.

Declaration of competing interest

The authors have declared no conflict of interest.

Acknowledgements

This work was supported by the Science and Technology Project of Guangdong Province (2015A020211005 and 2015B090901029) and the Fundamental Research Funds for the Central Universities (2019MS090).

References

[1] H. David, S. Liu, J.N. Miner, Urate handling in the human body, Curr. Rheumatol. Rep. 18 (6) (2016) 34–43.
[2] P.K. Tan, J.E. Farrar, E.A. Gaucher, et al., Coevolution of URAT1 and uricase during primate evolution: implications for serum urate homeostasis and gout, Mol. Biol. Evol. 33 (9) (2016) 2193–2200.
[3] A. Enomoto, M.F. Wempe, H. Tsuchida, et al., Molecular identification of a novel carnitine transporter specific to human testis - insights into the mechanism of carnitine recognition, J. Biol. Chem. 277 (39) (2002) 36262–36271.
[4] J.A. Singh, Emerging therapies for gout, Expet Opin. Emerg. Drugs 17 (4) (2012) 511–518.
[5] C.M. Burns, R.L. Wortmann, Gout therapeutics: new drugs for an old disease, Lancet 377 (9760) (2011) 165–177.
[6] S. Hania, J.A. Singh, Investigational drugs for hyperuricemia, Expet Opin. Invest. Drugs 24 (8) (2015) 1013–1030.
[7] P. Tristan, P. Richette, Investigational drugs for hyperuricemia, an update on recent developments, Expet Opin. Invest. Drugs 27 (5) (2018) 437–444.
[8] S.E. Sattui, A.L. Gaffo, Treatment of hyperuricemia in gout: current therapeutic options, latest developments and clinical implications, Therapeut. Adv. Musculoskelet. Dis. 8 (4) (2016) 145–159.
[9] P.K. Tan, T.M. Ostertag, J.N. Miner, Mechanism of high affinity inhibition of the human urate transporter URAT1[J], Sci. Rep. 6 (34995) (2016) 1–13.
[10] R. Nathan, S.E. Koch, M. Tranter, et al., The history and future of probenecid, Cardiovasc. Toxicol. 12 (1) (2012) 1–9.
[11] S.O. Ahn, S. Ohtomo, J. Kiyokawa, et al., Stronger uricosuric effects of the novel selective URAT1 inhibitor UR-1102 lowered plasma urate in tufted capuchin monkeys to a greater extent than benzbromarone, J. Pharmacol. Exp. Therapeut. 357 (1) (2016) 157–166.
[12] Hoy S.M. Lesinurad, First global approval, Drugs 76 (4) (2016) 509–516.

[13] S. Zancong, L.T. Yeh, K. Wallach, et al., In vitro and in vivo interaction studies between lesinurad, a selective urate reabsorption inhibitor, and major liver or kidney transporters, Clin. Drug Invest. 36 (6) (2016) 443–452.
[14] H.Y. Zhou, Y.Y. Li, J. Li, 3D-QSAR analysis of naphthyltriazole (lesinurad) analogs as potent inhibitors of urate transporter 1, Chin. J. Struct. Chem. 39 (3) (2020) 421–436.
[15] J.W. Wu, Y. Ling, Y.Q. Liu, et al., Synthesis, biological evaluation and 3D-QSAR studies of 1,2,4-triazole-5-substituted carboxylic acid bioisosteres as uric acid transporter 1 (URAT1) inhibitors for the treatment of hyperuricemia associated with gout, Bioorg. Med. Chem. Lett 29 (3) (2019) 383–388.
[16] S. Shyam, D. Bahulayan, Chemistry, chemical biology and photophysics of certain new chromene-triazole-coumarin triads as fluorescent inhibitors of CDK2 and CDK4 induced cancers, New J. Chem. 43 (35) (2019) 13863–13872.
[17] B. Lucka, V. Herzig, G.F. King, et al., Development of high-throughput fluorescent-based screens to accelerate discovery of P2X inhibitors from animal venoms, J. Nat. Prod. 82 (9) (2019) 2559–2567.
[18] R. Rick, R. Nowotny, C.W. Gertzen, et al., Fluorescent analogs of peptoid-based HDAC inhibitors: synthesis, biological activity and cellular uptake kinetics, Bioorg. Med. Chem. 27 (19) (2019) 115039–115048.
[19] Z.Y. Tang, Y. Zhang, Y.T. Chen, et al., The first small fluorescent probe as tyrosyl-DNA phosphodiesterase 1 (TDP1) substrate, Dyes Pigments 169 (18) (2019) 45–50.
[20] T. Cihlar, E. Ho, Fluorescence-based assay for the interaction of small molecules with the human renal organic anion transporter 1, Anal. Biochem. 283 (1) (2000) 49–55.
[21] L.P. Sullivan, J.A. Grantham, L. Rome, et al., Fluorescein transport in isolated proximal tubules in vitro-epifluorometric analysis, Am. J. Physiol. 258 (1) (1990) F46–F51.
[22] H.Y. Zhou, X.L. Li, Y.Y. Li, et al., Synthesis and bioevaluation of 1-phenylimidazole-4-carboxylic acid derivatives as novel xanthine oxidoreductase inhibitors, Eur. J. Med. Chem. 186 (2020) 111883–111898, 2020.